Journal of
Stem Cell Research & Therapy
ISSN: 2157-7633

El-Mahalaway et al., J Stem Cell Res Ther 2018, 8:6
DOI: 10.4172/2157-7633.1000431

Research Article Open Access

# Comparative Light and Electron Microscopic Study on the Therapeutic Efficacy of Adipose Derived Stem Cells Versus Exosomes for Experimentally Induced Acute Corneal Injuries in Rats

**Abeer M El-Mahalaway[1], Nahla El-Eraky El-Azab[1*], Mohamed Abdrabbo[2], Omar M Said[2], Dina Sabry[3] and Mohamed M El Sibaie[3]**

[1]*Department of Histology and Cell Biology, Benha Faculty of Medicine, Benha University, Benha, Egypt*
[2]*Department of Ophthalmology, Benha Faculty of Medicine, Benha University and Fayoum Faculty of Medicine, Fayoum University, Egypt*
[3]*Department of Medical Biochemistry and Molecular Biology, Faculty of Medicine, Cairo University, Cairo, Egypt*

## Abstract

**Background:** Corneal alkali injuries are considered a common ophthalmologic emergency with many serious complications. Adipose Tissue-Derived Stem Cells (ADSCs) and Mesenchymal Stem Cells derived Exosomes (MSCs-EX) are promising approaches in regenerative therapies.

**Objective:** The aim of this study is to evaluate the efficacy of ADSCs versus MSCs-EX on experimentally alkali-induced corneal injuries in rats.

**Materials and Methods:** 40 adult male albino rats were divided into four groups, that is, Group I: control rats, Group II: alkali burn rats, Group III: ADSCs treated rats after corneal alkali burn, Group IV: MSCs-EX treated rats after corneal alkali burn. Cornea specimens were taken and processed for histological examination.

**Results:** Group II showed obvious changes such as erosion with focal loss of some superficial epithelial cells, while the basal and intermediate epithelial cell layers had vacuolated cytoplasm with pyknotic nuclei. The substantia propria contained irregularly arranged collagen fibers with wide spacing, keratocytes, and congested blood vessels. Descemet's membrane appeared thin and degenerated with focal loss of some endothelial cells. Ultrastructural examination showed degenerated apical squamous cells with loss of microvilli on their free surface. The basal cells had irregular contour with widening of intracellular space between cells with multiple cytoplasmic vacuoles. The substantia propria showed disorganized collagen fibers with degenerated keratocytes and mononuclear cellular infiltration. Groups III and IV showed improvement of the histological and electron microscopic changes described in group II.

**Conclusion:** ADSCs and MSCs-EX can improve corneal alkali burn injuries and prevent their complications. Exosomes are a more promising therapeutic approach.

**Keywords:** Alkali burn; Cornea; Exosomes; Substantia propria; Keratocytes

**Abbreviations:** ADSCs: Adipose Tissue-Derived Stem Cells; MSCs-EX: Mesenchymal Stem Cells derived Exosomes; CNV: Corneal Neovascularization; FACS: Fluorescence-Activated Cell Sorting; PBS: Phosphate Buffer Saline; TEM: Transmission Electron Microscope; SD: Standard Deviation; VEGF: Vascular Endothelial Growth Factor; MMPs: Matrix Metalloproteinases.

## Introduction

Cornea is a specialized transparent avascular tissue that has a dome-shaped structure with smooth surface and it is formed of three functional layers. The location of the cornea is over the pupil, the iris, and the anterior chamber of the eye [1,2]. It provides a clear vision by refracting light onto the lens and centralizing on the retina. Cornea protects the eye against infections, abrasions, and structural damage to deeper tissues [3,4]. It contains self-renewal cells that have massive regeneration capacity. After minor scratches, the cornea can improve quickly; otherwise the deeper scars can lose their transparency and disturb the vision [4].

Corneal damage can be induced through many factors such as chemical, mechanical, or thermal injury. Chemical injuries, especially those produced by alkaline agents, are a worldwide common cause of ophthalmologic emergency especially in developing countries in young age groups [5,6].

The approaches to the treatment of corneal alkali burn are based on using one member of the following medical and operative therapeutic strategies such as steroids, non-steroidal anti-inflammatory agents, citrate, argon laser photocoagulation, photodynamic therapy, artificial tears, collagenase inhibitors, therapeutic contact lenses, topical fibronectin, conjunctival transplantation, amniotic membrane repairing and limbal transplantation. Occasionally, these therapies are ineffective, particularly for large inflammatory Corneal Neovascularization (CNV) and thus insight is directed towards alternative treatment modalities for eliminating those dangerous drawbacks [7,8].

ADSCs are a new type of MSCs that are plentiful in individuals. They include a type of multipotent adult stem cells isolated from adipose tissue and have the capacities of self-regeneration and differentiation

***Corresponding author:** Nahla El-Eraky El-Azab, Department of Histology and Cell Biology, Benha Faculty of Medicine, Benha University, Benha, Egypt, Tel: +201027636357; E-mail: eleraky_nahla@yahoo.com/nahla.Eleraky@fmed.bu.edu.eg

**Received** June 20, 2018; **Accepted** July 09, 2018; **Published** July 13, 2018

**Citation:** El-Mahalaway AM, El-Azab NEE, Abdrabbo M, Said OM, Sabry D, et al. (2018) Comparative Light and Electron Microscopic Study on the Therapeutic Efficacy of Adipose Derived Stem Cells Versus Exosomes for Experimentally Induced Acute Corneal Injuries in Rats. Stem Cell Res Ther 8: 431. doi: 10.4172/2157-7633.1000431

into various cell lineages [9,10]. Both BMSCs and ADSCs have common biological properties such as cell surface markers, gene expression profile, immunosuppressive features, and differentiation capacity, but ADSCs have more proliferative capacity than that of BMSCs [11]. ADSCs have been used in a recent technique for wound repair, regeneration, and tissue engineering procedures because the adipose tissue is easy to gain and process; in addition, the isolated cells expand rapidly and differentiate into different cell types *in vitro* [12-14].

Exosomes are products of endocytosis. They are small vesicles with a bilipid membrane, their diameter ranges from 30-150 nm, and they have abundant proteins, lipids, mRNAs, and microRNAs for transmitting hereditary information [15,16]. They are released by all cell categories and found in blood, urine, breast milk and play valuable role in intercellular communication by protein and RNA delivery [17,18]. They are released physiologically under ordinary circumstances, but their rate of release is increased under pathological states such as degeneration and tumors [19]. Nowadays, exosomes have a vital role in treatment of many diseases such as liver fibrosis, acute kidney injury, myocardial infarction, ischemia induced neural degeneration and wound repair [20].

The aim of the study is to evaluate the efficacy of ADSCs versus MSCs-EX on experimentally alkali-induced corneal injuries in rats.

## Materials and Methods

40 adult male rats of average weight 150-200 g were utilized in this study. Rats were held in the laboratory animal house unit of Kasr Al-Ainy Faculty of Medicine, Cairo University, Cairo, Egypt. Strict maintenance and cleaning measures were applied to keep the animals in a normal healthy state. They were housed in animal cages at room temperature (25 ± 1°C) and relative humidity (55 ± 5) with 12 hrs light/12 hrs dark cycle and nourished balanced diet and water ad libitum. All ethical rules for animal treatment were followed and were managed via the animal facilities. The experimental protocol was approved by the Institutional Animal Care Committee of Cairo University, Cairo, Egypt.

### Isolation, phenotype and features of ADSCs

ADSCs were prepared from adipose tissue gained from flanks and inguinal areas of healthy 9 week-old rats (n=10). Adipose tissue was hydrolysed by collagenase type II (Sigma, USA) liquefied in Phosphate Buffer Saline (PBS); Gibco/Invitrogen, Grand Island, New York, USA) for 2 hrs at 37°C. 2 µm filters were used to eliminate all tissue debris, followed by centrifugation at 1,000 rounds per minute (rpm) for 5 min to form a cell pellet which was cultured with a RPMI medium (Gibco BRL, USA) and 10% fetal bovine serum (FBS, Gibco BRL, USA). The culture was humidified in a cell culture incubator containing 5% carbon dioxide at 37°C. At 70-90% adipose MSCs confluence, it was separated with 0.25% trypsin-EDTA (Gibco BRL, USA) and resuspended in other flasks. Fourth-passage ADSCs were applied in the whole experiments. The ADSCs were characterized in culture by their morphology, spindle-shaped cells. Additional identification of adipose MSCs was established by identification of CD29 and CD44 surface markers using flow cytometry (Beckman Coulter) [13,21].

### Isolation and identification of MSCs-EX

Exosomes were prepared from supernatants of fourth-passage MSCs ($5 \times 10^6$ /ml) cultured in RPMI supplemented with 0.5% of Bovine Serum Albumin (BSA) (Sigma-Aldrich, St. Louis, MO, USA). Debris was isolated through centrifugation at 2000 g for 20 min. Further centrifugation of the cell-free supernatants was done at 100,000 g (Beckman Coulter Optima L 90K ultracentrifuge) for 1 hr at 4°C, followed by washing in serum-free medium 199 containing chemical buffering agent, and more ultracentrifugation in the same pervious circumstances was performed. The protein content of the exosomes was deliberated using the Bradford method (Bio Rad, Hercules, CA, USA). Purified exosomes were cultured overnight in the medium used for their collection. Microscopic identification and photographing of exosomes were done by utilizing the Jeol Transmission Electron Microscope (TEM) 300 system. Flow cytometry was performed for Fluorescence-Activated Cell Sorting (FACS). The FITC conjugated antibodies, CD73 (Becton Dickinson, FACS Calibur) and CD81 (Miltenyi Biotec, Bergisch Gladbach, German) were utilized [22,23].

### Transmission Electron Microscope (TEM) of MSCs-EX

Exosomes were gently placed on Formvar-coated copper grids. They were allowed to be adsorbed for 45 min and then handled for standard uranyl acetate staining. The grids were irrigated with PBS three times and left to semidry at room temperature prior to examining in TEM. Images were obtained by using TEM JEOL (JEM-2100; Akishima, Tokyo, Japan) at an accelerating voltage of 80 kV [19].

### Labelling of ADSCs with PKH26 dye

ADSCs were harvested in the fourth passage and labelled with the PKH26 (Sigma-Aldrich, St. Louis, MO, USA) [5]. Fluorescent linker dye PKH26 is a red fluorochrome having 551 nm excitation and 567 nm emission that binds irreversibly to cell membranes. Cells were centrifuged and washed twice in a serum-free medium. They were pelleted and suspended in stain solution.

### Labelling MSCs-EX with PKH26 dye

Fluorescent labelling of exosomes with the PKH26 dye was carried out according to a procedure previously reported by Hajrasouliha [24], by using a commercially ready kit (Sigma-Aldrich, St. Louis, MO, USA) according to the manufacturer's directions.

### Tracking of ADSCs and MSCs-EX

Fluorescent-labelled ADSCs and MSCs-EX were detected in cornea cryosections using fluorescence microscope (Leica Microsystems CMS GmbH, Wetzlar, Germany). This was done in the Biochemistry Department, Faculty of Medicine, Cairo University.

### Induction and evaluation of corneal alkali injury

Animals were anesthetized by intramuscular injection of 0.5 mg/kg ketamine. After that, corneal alkali burn was induced on the right eye of each rat, and the other eye was left without burn for allowing the animals to eat and move freely. A disc of Whatman® filter paper (4 mm in diameter, Sigma-Aldrich Corp., Madrid, Spain, cat. No. WHA10016508) was soaked in 1% NaOH (4 ml) (Sigma Aldrich, Darmstadt, Germany) and then inserted on the whole cornea for 25 seconds; it was then irrigated with 10 ml of distilled water for one minute. The corneal epithelial defect was stained with a topically applied fluorescein. The stained corneal ulcers were examined under a cobalt blue light source from a direct ophthalmoscope (Welch Allyn, Skaneateles Falls, NY, USA) to evaluate the degree of the corneal epithelial defect [25].

## Experimental Design

Animals were divided into four groups, 10 rats each.

**Group I (control group):** The animals of this group were divided equally into two subgroups.

Subgroup Ia: The corneas of the rats were not injured but were irrigated with distilled water.

Subgroup Ib: Each rat received single sub-conjunctival injection of equivalent volume of 0.2 ml PBS, a vehicle of ADSCS and exosomes.

**Group II (alkali burn group):** A corneal alkali burn was induced in the right eye of each rat.

**Group III (ADSCs group):** 24 hrs following the corneal alkali burn, the rats were injected sub-conjunctivally with a single dose of 1.3 × $10^5$ cultured and labelled ADSCs suspended in 0.2 ml PBS [26].

**Group IV (MSCs-EX group):** One day after corneal alkali burn, the rats were injected sub-conjunctivally with 20 µg PKH26 labelled MSCs-EX diluted with the same amount of PBS every other day [27].

The rats of all groups were killed two weeks later by ether inhalation, the eyeballs were enucleated rapidly, and then the corneas were carefully dissected. Pieces of the corneas were put in 10% neutral-buffered formalin (Sigma-Aldrich St. Louis, MO, USA) and processed for light microscopic study. Paraffin sections (4-5 µm thick) were prepared and stained with H&E stains (Sigma-Aldrich St. Louis, MO, USA) for the histological examination of the cornea [28].

### Transmission Electron Microscopic (TEM) study

Small pieces (1 $mm^3$) from the cornea of right side were collected and ultrathin sections were prepared according to Hayat [29], in Tanta EM Unit, Faculty of Medicine, Tanta University, Tanta, Egypt. Sections were photographed using a TEM (JEM-2100; Akishima, Tokyo, Japan) at the Faculty of Medicine, Benha University, Benha, Egypt.

### Morphometric analysis

Using a Leica Qwin 500 image analysis computer system (Leica Microsystems Ltd, Cambridge, UK) at the Pathology Department, Faculty of Medicine, Cairo University, ten slides from each group were checked. On each slide, 10 non-overlapping fields were assessed to measure the corneal epithelial thickness (µm). Corneal thickness of epithelium was studied at a magnification of × 630.

### Real Time PCR (q RT-PCR)

Corneal tissues of all studied groups were lysed and total RNA was separated with RNeasy Mini Kit (Qiagen) and further analysed for quantity and quality with Beckman dual spectrophotometer (USA) [30].

For assessment of quantitative expression of IL-1β, TNF-α, and VEGF, the subsequent procedure was followed. 10 ng of the total RNA from every sample was used for cDNA synthesis by reverse transcription using High Capacity cDNA Reverse Transcriptase Kit (Applied Biosystem, USA). Later on, the cDNA was amplified with the Sybr Green I PCR Master Kit (Fermentas) in a 48-well plate using the Step One instrument (Applied Biosystem, USA) as follows: 10 min at 95°C for enzyme activation, then 40 cycles of 15 seconds at 95°C, 20 seconds at 55°C and finally 30 seconds at 72°C for the amplification stage. Changes in the expression of each target gene were normalized in proportion to the mean Critical Threshold (CT) values of GAPDH as a housekeeping gene by the ΔΔCt method. We used 1 µM of both primers specific for each target gene. Primers sequence and annealing temperature specific for each gene are demonstrated in Table 1.

### Statistical analysis

All the data collected from the experiment were recorded and analysed using IBM SPSS software for Windows, Version 20 (IBM Corp., Armonk, NY, USA). One-way Analysis of Variance (ANOVA) with post hoc Scheffe's test was used to contrast differences between the groups. In each test, the data expressed as the mean (M) value, Standard Deviation (SD) and differences were considered significant at $P<0.01$.

## Results

### Histological study

**ADSCs and MSCs-EX characterization and homing:** ADSCs were recognized at 10-day culture by inverted microscope as adherent spindle-shaped cells with some polyhedral cells in between (Figure 1a). FACS analysis for ADSCs characterization was done. ADSCs showed 99.72% positivity for CD29 and 99.67% positivity for CD44 (Figure 1b). ADSCs labelled with PKH26 fluorescent dye were identified *in vitro* by means of a fluorescent microscope (Figure 1c). ADSCs labelled with PKH26 fluorescent dye were recognized in cornea by their strong red fluorescence using fluorescent microscope (Figure 1d). DAPI stained ADSCs nuclei were identified in cornea by their blue fluorescence with fluorescent microscope (Figure 1e). TEM of MSCs-EX showed spheroids appearance with diameter less than 100 nm (Figure 2a). MSCs-EX labelled with PKH26 fluorescent dye were recognized *in vitro* and in cornea using a fluorescent microscope as strong red fluorescence (Figures 2b and 2c).

### H&E results

Group I (control groups): All the subgroups showed identical histological picture. The sections of the control rats showed ordinary histological landmarks of the cornea consisting of five distinct layers. The outer layer was stratified squamous non-keratinized epithelium with smooth regular upper surface formed of superficial flattened squamous cells, a middle layer of two rounded cells, and one layer of basal columnar cells resting on a thin intact Bowman's membrane which is a thin homogenous acidophilic layer. Intermediate substantia propria was composed of normal organized collagen fibers with spindle-shaped keratocytes in between. Next layers were endothelial cells with flat nuclei resting on Descemet's membrane (Figure 3a).

| Target gene | Primer sequence: 5`- 3` | Gene bank accession number |
|---|---|---|
| IL-1β | F: GCTGTGGCAGCTACCTATGTCTTG | NM031512.2 |
| | R: AGGTCGTCATCATCCCACGAG | |
| TNF-α | F: AACTCGAGTGACAAGCCCGTAG | XM_008772775.2 |
| | R: GTACCACCAGTTGGTTGTCTTTGA | |
| VEGF | F:GTGGACATCTTCCAGGAGTA | XM011354722.1 |
| | R:TCTGCATTCACATCTGCTGT | |
| GAPDH | F:CACCCTGTTGCTGTAGCCATATTC | XR598347.1 |
| | R:GACATCAAGAAGGTGGTGAAGCAG | |

**Table 1:** Primers sequence and annealing temperature specific for each gene.

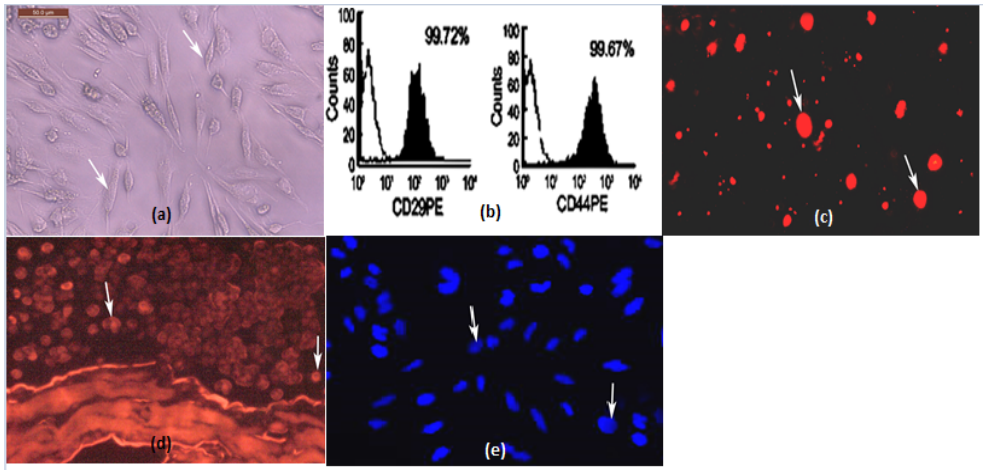


**Figure 1: (a)** Inverted microscope micrograph of a primary culture of adipose stem cells at 10-day culture. The cultured undifferentiated ADSCs are adherent spindle-shaped cells (white ↑) **(× 200)**; **(b)** FACS analysis for ADSCs characterization showing 99.72% positivity for CD29 and 99.67% positivity for CD44; **(c)** A fluorescent microscope photograph showing ADSCs labelled with PKH26 fluorescent dye *in vitro* (arrows) **(× 1000)**; **(d)** A fluorescent microscope photograph showing ADSCs labelled with PKH26 fluorescent dye in cornea (arrows) **(× 1000)**; **(e)** A fluorescent microscope photograph showing ADSCs nuclei labelled with DAPI in cornea (arrows) **(× 1000**).

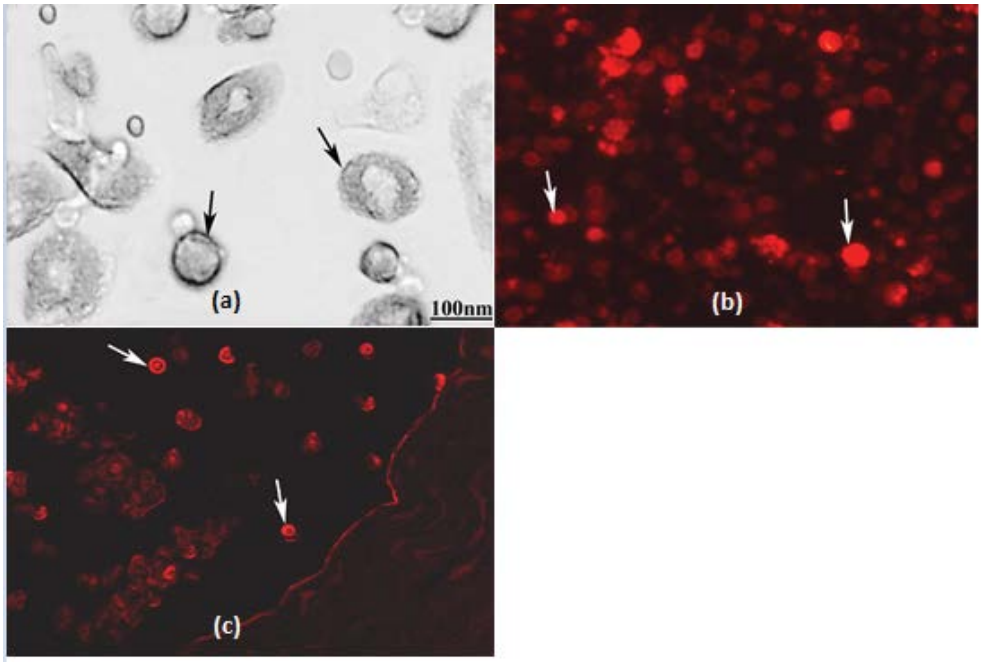


**Figure 2: (a)** Electron micrograph of exosome showing spheroid appearance (black arrows) **(100 nm)**; **(b)** A fluorescent microscope photograph showing exosome labelled with PKH26 fluorescent dye *in vitro* (arrows) **(× 1000)**; **(c)** A fluorescent microscope photograph showing homing of exosome labelled with PKH26 fluorescent dye in cornea (arrows) **(× 1000)**.

Group II (alkali burn group): This group showed many obvious histological changes such as erosion with loss of some superficial epithelial cells in some areas. Most of the basal and intermediate epithelial cells had vacuolated cytoplasm with pyknotic or karyolytic nuclei. Bowman's membrane was very thin and substantia propria contained collagen fibers with wide spaces and degenerated keratocytes in between. The presence of inflammatory cells and congested blood vessels was noted. Descemet's membrane appeared thin and degenerated with focal loss of some endothelial cells (Figure 3b). The corneal epithelial layer was disorderly arranged and had vacuolated cytoplasm. Bowman's membrane was very thin and substantia propria contained irregularly arranged collagen fibers with wide spacing, keratocytes, and congested blood vessels in between (Figure 3c).

Group III (ADSCs group): This group showed incomplete restoration of surface epithelium with thin intact Bowman's membrane. Substantia propria consisted of collagen fibers with narrow spaces and keratocytes in between. Descemet's membrane was lined by a single layer of flattened endothelial cells (Figure 3d).

Group IV (MSCs-EX group): It showed regeneration of corneal epithelium with thin intact Bowman's membrane. Substantia propria had regularly arranged collagen fibers, narrow spaces, and normal keratocytes in between. Descemet membrane and endothelial cells were apparently normal (Figure 3e).

## EM results

TEM examination of superficial layers of the corneal epithelium from Group I showed squamous cell with flat nucleus and minute microvilli on the free surface. The numerous desmosomes connecting cells together were noticed (Figure 4a). Group II revealed erosion and loss of superficial squamous cell with loss of microvilli on the free surface, multiple vacuolations and widening of intracellular space. Hyperchromatic shrunken nucleus of intermediate epithelial layer was also seen (Figure 4b). Group III showed nearly normal superficial squamous cell with flat nucleus, apical microvilli, few vacuolations and slight widening of intracellular spaces (Figure 4c). Group IV showed nearly normal superficial squamous cell with flat nucleus and apical microvilli and electron-dense desmosomes connecting cells with narrow intracellular space (Figure 4d).

Ultra-structural examination of the basal cell layers of the corneal epithelium from Group I showed columnar cell with euchromatic nucleus, prominent nucleolus and straight regular basal lamina laying below the epithelium. The cells were attached to the basal lamina with hemidesmosomes that looked like dotted electron-dense spots (Figures 5a and 5b). Group II showed irregular contour of a part of a columnar cell and a portion of its nucleus appeared dark with many vacuoles in its cytoplasm. The basal lamina existed beneath the basal corneal epithelium with interrupted hemidesmosome junctions (Figure 5c). Group III exhibited nearly normal columnar cells with euchromatic nuclei and basal lamina present beneath the basal corneal epithelium. The cells were joined to the basal lamina with hemidesmosomes that looked like dotted electron-dense spots (Figure 5d). Group IV revealed nearly normal columnar cell with euchromatic nucleus. The basal lamina was regular and was located under the basal corneal epithelium. The cells were linked to the basal lamina with hemidesmosomes that appeared as dotted electron-dense spots (Figure 5e).

Electron microscopic examination of the substantia propria from Group I presented a spindle-shaped keratocyte with euchromatic nucleus and scanty cytoplasm containing cell organelles. The collagen fibers appeared regularly arranged in longitudinal and transverse planes (Figure 6a). Group II showed degenerated keratocytes with shrunken nuclei, little cytoplasm, and few cytoplasmic processes. The wide spaces among the collagen fibers and keratocyte were seen (Figure 6b). Irregularly arranged collagen fibers and an irregular eosinophil with bilobed nucleus and granular cytoplasm were obvious in the stroma (Figure 6c). There was mononuclear cellular infiltration predominantly in macrophages with characteristic pseudopodia, apoptotic bodies and multilobed nucleus. Degenerated keratocytes with shrunken nuclei and vacuoles were seen in the disorganized collagen of the corneal stroma

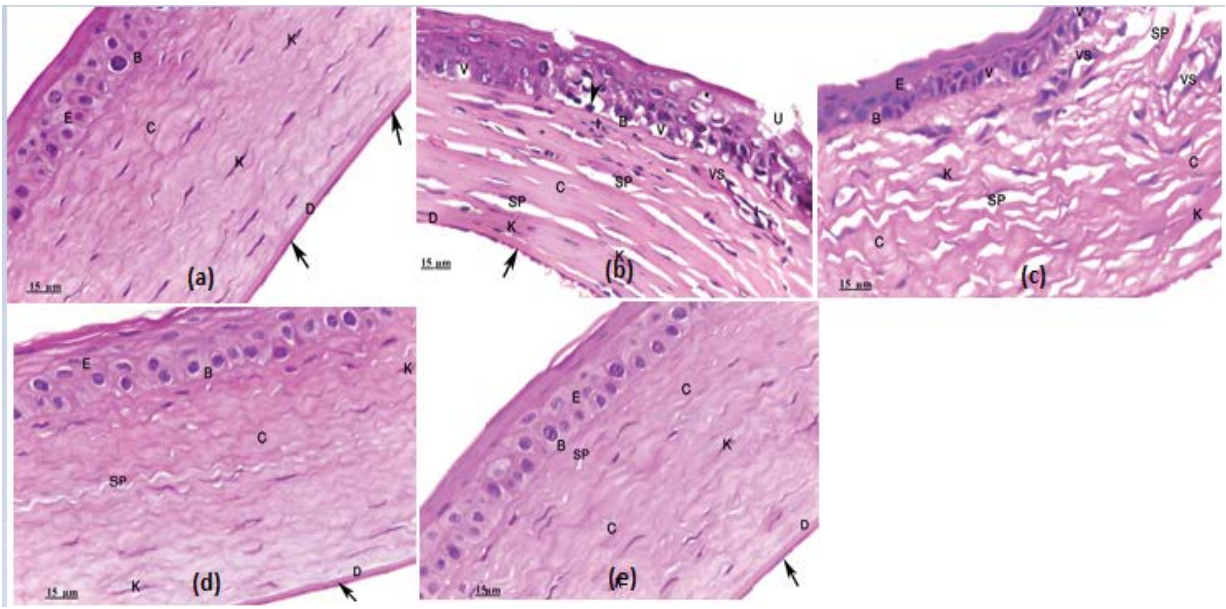


**Figure 3: (a)** A photomicrograph of a section in the cornea of Group I showing stratified squamous nonkeratinized epithelium (E) resting on a thin homogenous acidophilic Bowman's membrane layer (B). Regularly arranged collagen fibers (C) with spindle-shaped keratocytes (K) in between were observed. Notice endothelial cells (black arrow ↑) with flat nuclei resting on Descemet's membrane (D) **(H&E × 630, scale bar=15 µm)**; **(b)** A photomicrograph of a section in the cornea of Group II showing erosion with focal loss of some superficial epithelial cells (U). Most of the basal and intermediate epithelial cells have vacuolated cytoplasm (V) with pyknotic (▲arrow heads) or karyolytic (*) nuclei. Bowman's membrane is very thin (B). Substantia propria shows collagen fibers (C) with wide spaces (SP) and keratocytes (K) in between. Notice the presence of inflammatory cells (I) and congested blood vessels (VS). Descemet's membrane (D) appears thin and degenerated with focal loss of some endothelial cells (black arrow) **(H&E × 630, scale bar=15 µm)**; **(c)** A photomicrograph of a section in the cornea of Group II showing disorderly arranged epithelial layer (E) and some of the cells have vacuolated cytoplasm (V). Bowman's membrane is very thin (B). Substantia propria shows irregularly arranged collagen fibers (C) with wide spaces (SP) and keratocytes (K) in between. Notice congested blood vessels (VS) **(H&E × 630, scale bar=15 µm)**; **(d)** A photomicrograph of a section in the cornea of group III showing incomplete restoration of surface epithelium (E) with thin intact Bowman's membrane (B). Substantia propria displays regularly arranged collagen fibers (C) with narrow spaces (SP) and keratocytes (K) in between. Descemet's membrane (D) is lined with a single layer of flattened endothelial cells (black arrow ↑) **(H&E × 630, scale bar=15 µm)**; **(e)** A photomicrograph of a section in the cornea of Group IV showing complete regeneration of corneal epithelium (E) with thin intact Bowman's membrane (B). Substantia propria shows regularly arranged collagen fibers (C), narrow spaces (SP), and normal keratocytes (K) in between. Descemet's membrane (D) and endothelial cells (black arrow ↑) are nearly normal **(H&E × 630, scale bar=15 µm)**.

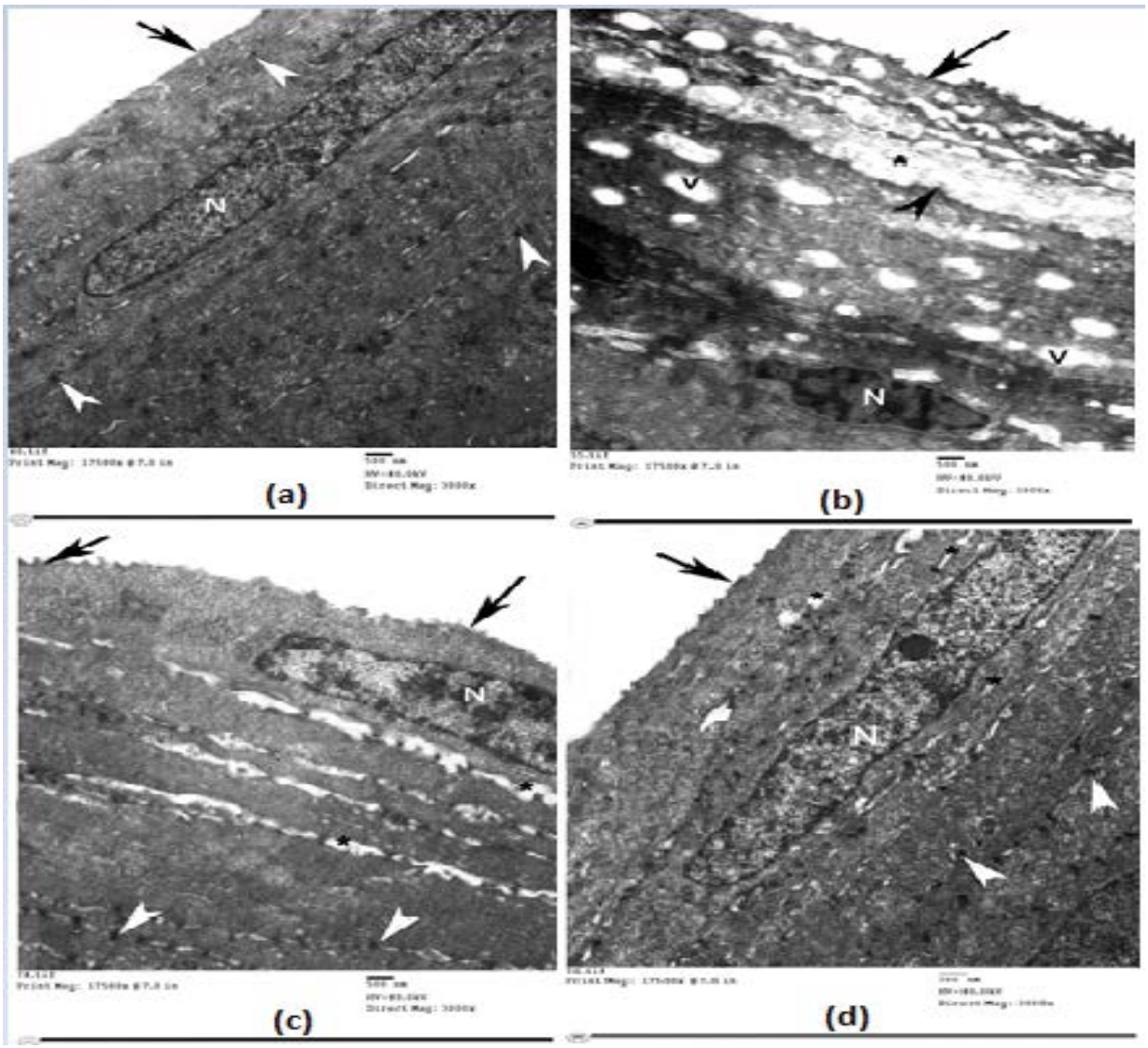


**Figure 4: (a)** An electron micrograph of a section in the cornea of Group I showing superficial squamous cell with flat nucleus (N) and minute microvilli (black arrow ↑) on the free surface. Notice the numerous desmosomes (▲ white arrow heads) **(TEM, × 3000)**; **(b)** An electron micrograph of a section in the cornea of Group II showing erosion and loss of superficial squamous cell with loss of their microvilli (black arrow ↑) on the free surface. Notice multiple vacuolations (V) and widening of intracellular space (*) (▲ black arrow heads). Hyperchromatic shrunken nucleus (N) of intermediate epithelial layer is seen **(TEM, × 3000)**; **(c)** An electron micrograph of a section in the cornea of Group III showing nearly normal superficial squamous cell with flat nucleus (N) and apical microvilli (black arrow ↑). Notice desmosomes (▲ white arrow heads) and narrow intracellular space (*) **(TEM, × 3000)**; **(d)** An electron micrograph of a section in the cornea of Group IV showing nearly normal superficial squamous cell with flat nucleus (N) and apical microvilli (black arrow ↑). Notice electron-dense desmosomes (▲ white arrow heads) with narrow intracellular space (*) **(TEM, × 3000)**.

(Figure 6d). Group III showed narrow spaces in between regularly arranged collagen fibers of the corneal stroma and long keratocyte with its nucleus and parallel cisternae of rough endoplasmic reticulum (Figure 6e). Group IV revealed regular arrangement of collagen fibers of the corneal stroma and long, slender keratocytes with their nuclei and parallel cisternae of rough endoplasmic reticulum (Figure 6f).

Ultra-structural examination of Descemet's membrane and endothelial cell layer from Group I revealed a thick homogenous electron-dense non-cellular membrane on which endothelial cells were resting. The endothelial cell layer had a moderate electron-dense nucleus and cytoplasm with variable-sized pinocytotic vesicles (Figure 7a). Group II showed a portion of Descemet's membrane lined with swollen endothelial cell. The endothelial cell had many variable-sized cytoplasmic vacuoles, degenerated mitochondria and an electron-dense elongated nucleus (Figure 7b). In Group III, there was a thick homogenous electron-dense Descemet's membrane lined with a nearly normal endothelial cell with moderate electron-dense elongated nucleus and variable-sized pinocytotic vesicles (Figure 7c). Group IV revealed thick homogenous electron-dense Descemet's membrane lined with endothelial cells. There was a nearly normal endothelial cell with moderate electron-dense elongated nucleus and variable-sized pinocytotic vesicles (Figure 7d).

## Morphometric and statistical results

The mean and SD of corneal epithelium thickness for all groups

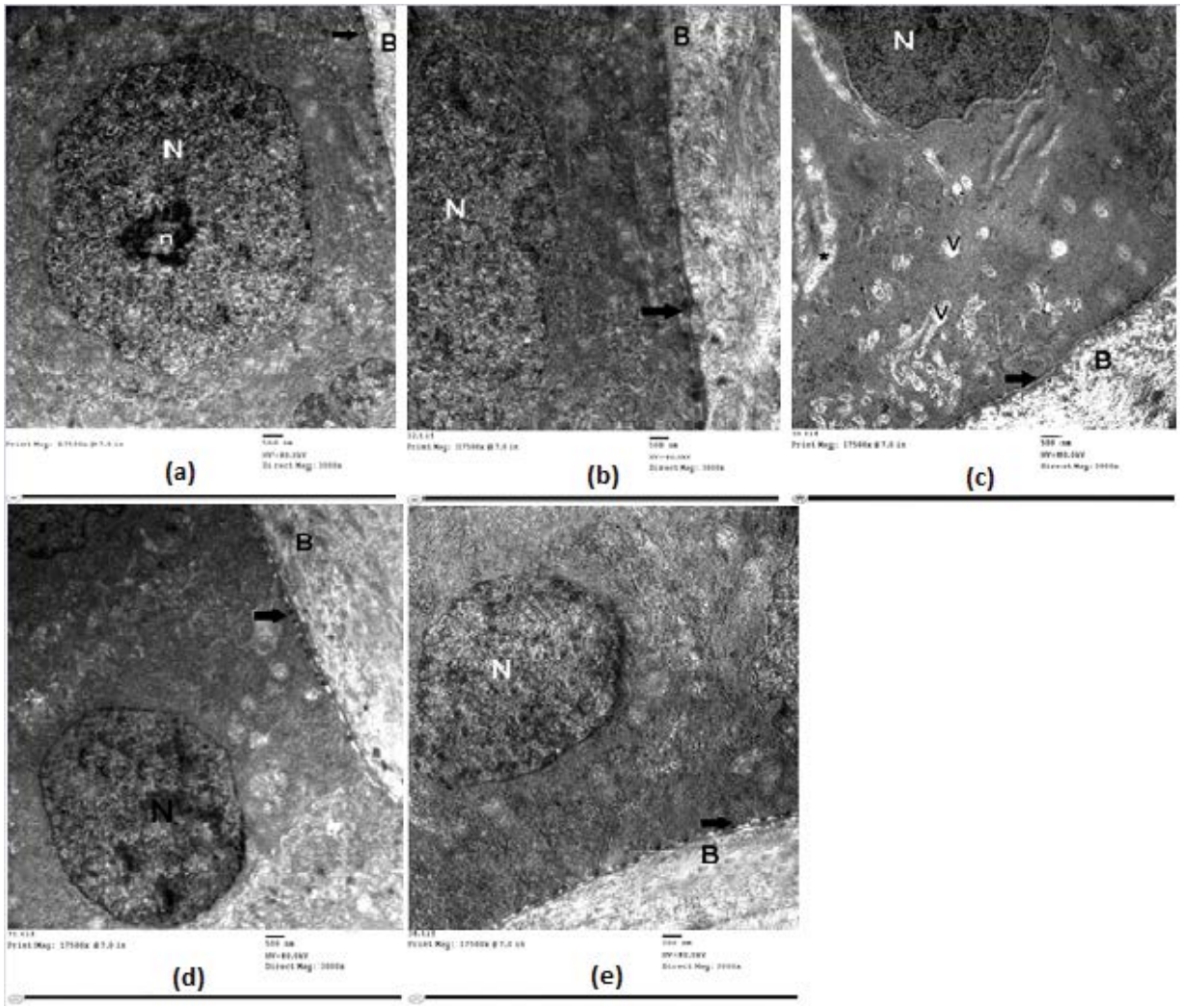


**Figure 5: (a)** An electron micrograph of a section in the cornea of Group I showing columnar cell of the basal layer of the corneal epithelium with euchromatic nucleus (N) and prominent nucleolus (n). Notice straight and regular basal lamina (B) and hemidesmosomes appear as dotted electron-dense spots (black arrow ↑). **(TEM, × 3000)**; **(b)** An electron micrograph of a section in the cornea of Group I showing part of columnar cell of the basal layer of the corneal epithelium with portion of its euchromatic nucleus (N). Notice straight and regular basal lamina (B) and hemidesmosomes appear as dotted electron-dense spots (black arrow ↑) **(TEM, × 3000)**; **(c)** An electron micrograph of a section in the cornea of Group II showing irregular contour of a part of columnar cell of basal layer of the corneal epithelium with portion of its nucleus appearing dark (N). Many vacuoles are seen in its cytoplasm (V). Notice basal lamina (B) and interrupted hemidesmosomes (black arrow ↑). Widening of intracellular space (*) is observed **(TEM, × 3000)**; **(d)** An electron micrograph of a section in the cornea of Group III showing nearly normal columnar cells of the basal layer of the corneal epithelium with euchromatic nucleus (N). Regular basal lamina (B) and electron-dense spots of hemidesmosomes are observed (black arrow ↑) **(TEM, × 3000)**; **(e)** An electron micrograph of a section in the cornea of Group IV showing nearly normal columnar cell of the basal layer of the corneal epithelium with euchromatic nucleus (N). Regular basal lamina (B) and electron-dense spots of hemidesmosomes are observed (black arrow ↑) **(TEM, × 3000)**.

were represented in Table 2 and Histogram 1. There was a significant increase in mean thickness of corneal epithelium ($P<0.01$) in Groups I, III, and IV compared with Group II. Group III and Group IV showed insignificant changes ($P<0.01$) compared with Group I.

The mean and SD of IL-1β, TNF-α, and VEGF genes expression for all groups were represented in Table 3 and Histogram 2. There was a significant increase in IL-1β, TNF-α, and VEGF genes expression in Group II compared with Group I ($P<0.01$), and there was a significant decrease in Groups III and IV compared with Group II ($P<0.01$). However, the reduction of the expression of VEGF was significant in Group IV compared to group III.

## Discussion

A chemical burn to the cornea is one the gravest ocular injuries resulting in extensive and permanent visual impairment. Therefore, it is necessary to use proper management for accurate duration. Alkali burns are the commonest method for researching of corneal ulceration in laboratory animals. Alkali injury causes a lot of serious complications such as corneal infection, ulceration, perforation, neovascularization (NV), opacification, disruption of the immunosuppressive microenvironment in the anterior chamber, severe adhesion of the eyelids and conjunctiva and finally decrease in visual acuity or blindness [6].

The light and electron microscopic examination of corneal sections

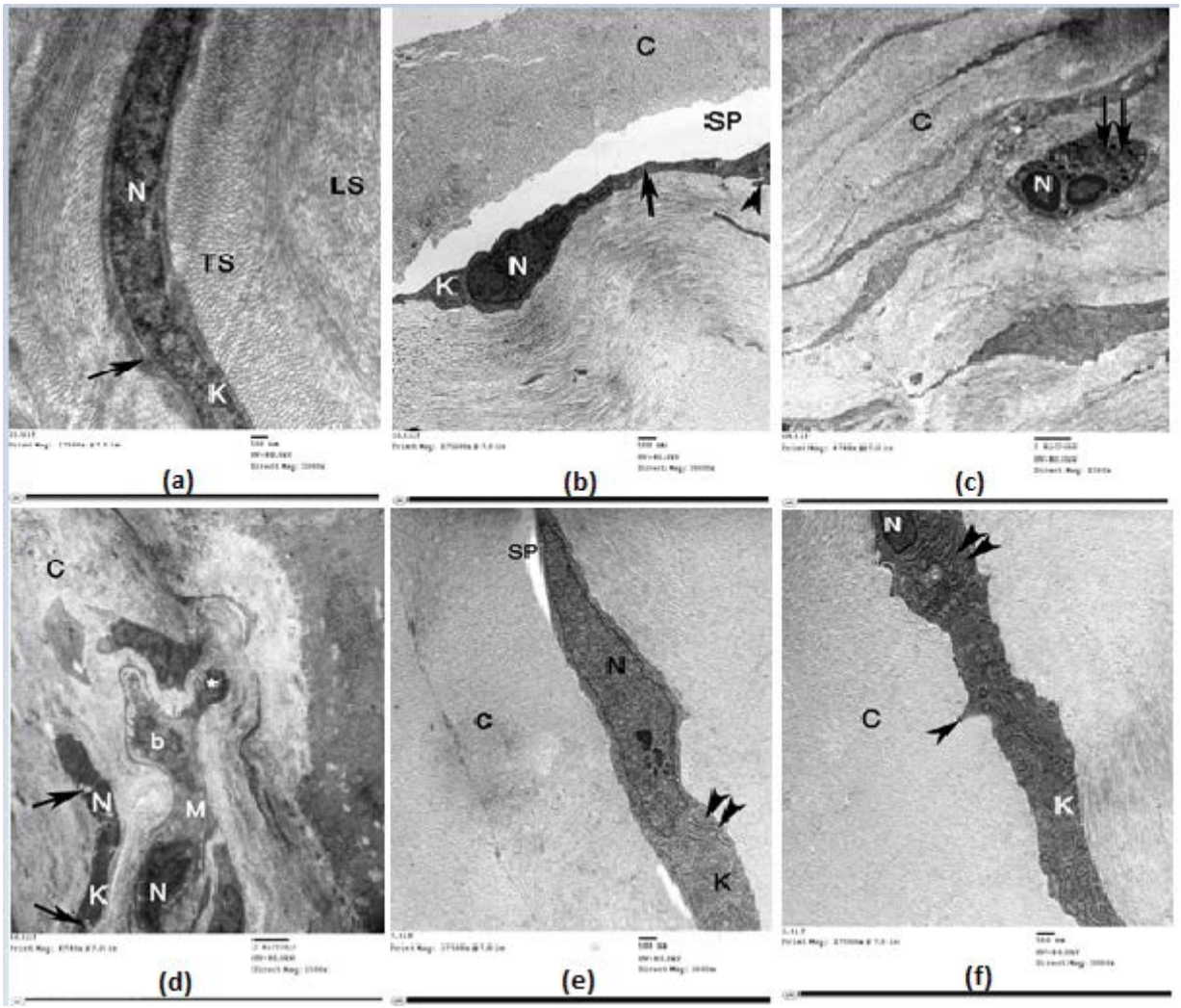


**Figure 6: (a)** An electron micrograph of a section in the cornea of Group I showing a spindle-shaped keratocyte (K) with euchromatic nucleus (N) and a scanty cytoplasm (black arrow ↑). The collagen fibers appear regularly arranged in longitudinal (LC) and transverse (TC) planes **(TEM, × 3000)**; **(b)** An electron micrograph of a section in the cornea of Group II showing the degenerated keratocytes (K) with shrunken dark nucleus (N), little cytoplasm (black arrow ↑), and cytoplasmic processes (▲ arrow heads). Notice the wide spaces (SP) in between the collagen fibers (C) and keratocyte **(TEM, × 3000)**; **(c)** An electron micrograph of a section in the cornea of Group II showing a large irregular eosinophil with bilobed nucleus (N) and granular cytoplasm (↑↑). Notice an irregular arrangement of the collagen fibers (C) in the stroma **(TEM, × 1500)**; **(d)** An electron micrograph of a section in the cornea of Group II showing mononuclear cellular infiltration predominantly in macrophages (M) with characteristic pseudopodia (*), phagocytic bodies (b), and multilobed nucleus (N). Notice the degenerated keratocytes (K) with shrunken nucleus (N) and vacuoles (black arrow ↑) in the disorganized collagen (C) of the corneal stroma **(TEM, × 1500)**; **(e)** An electron micrograph of a section in the cornea of Group III showing long keratocyte (K) with elongated nucleus (N) and parallel cisternae of rough endoplasmic reticulum (two arrow heads ▲▲). Notice the narrow spaces (SP) in between a regular arrangement of the collagen fibers (C) of the corneal stroma **(TEM, × 3000)**; **(f)** An electron micrograph of a section in the cornea of Group IV showing a regular arrangement of the collagen fibers (C) of the corneal stroma. Notice long, slender keratocytes (K) with part of its nucleus (N), cytoplasmic processes (▲ arrow heads), and parallel cisternae of rough endoplasmic reticulum (two arrow heads ▲▲) **(TEM, × 3000)**.

of Group II revealed several changes as erosion and focal loss of some superficial epithelial cells. Most of the basal and intermediate epithelial cells had vacuolated cytoplasm with pyknotic or karyolytic nuclei. Substantia propria showed widely spaced and disrupted collagen fibers with degenerated keratocytes in between. Mononuclear inflammatory cellular infiltration, irregular eosinophil, and congested blood vessel were also seen. Descemet's membrane was thin with degenerated and focal loss of some endothelial cells. There was a significant decrease in corneal epithelial thickness and significant increase in IL-1β, VEGF, and TNF genes expression as quantitated by RT-PCR in corneal tissue compered to Group II.

These results were in accordance with many researchers [3,5,14,31-33] who reported the presence of widely spaced and disrupted collagen fibers with degeneration and necrosis of keratocytes after damaging cornea with the irritants and alkalis.

Many reporters [25,33,34] clarified that alkali burns induced ulcers are accompanied with the existence of inflammatory cells infiltration in the corneal stroma, which are pointing to the inflammation. They lead to damage of the normal corneal architecture due to liberation of Matrix Metalloproteinases (MMPs) and several proteolytic enzymes that dissolve its collagen fibers. Neutrophils and macrophages infiltrate into the cornea after chemical burn as immune cells that are responsible

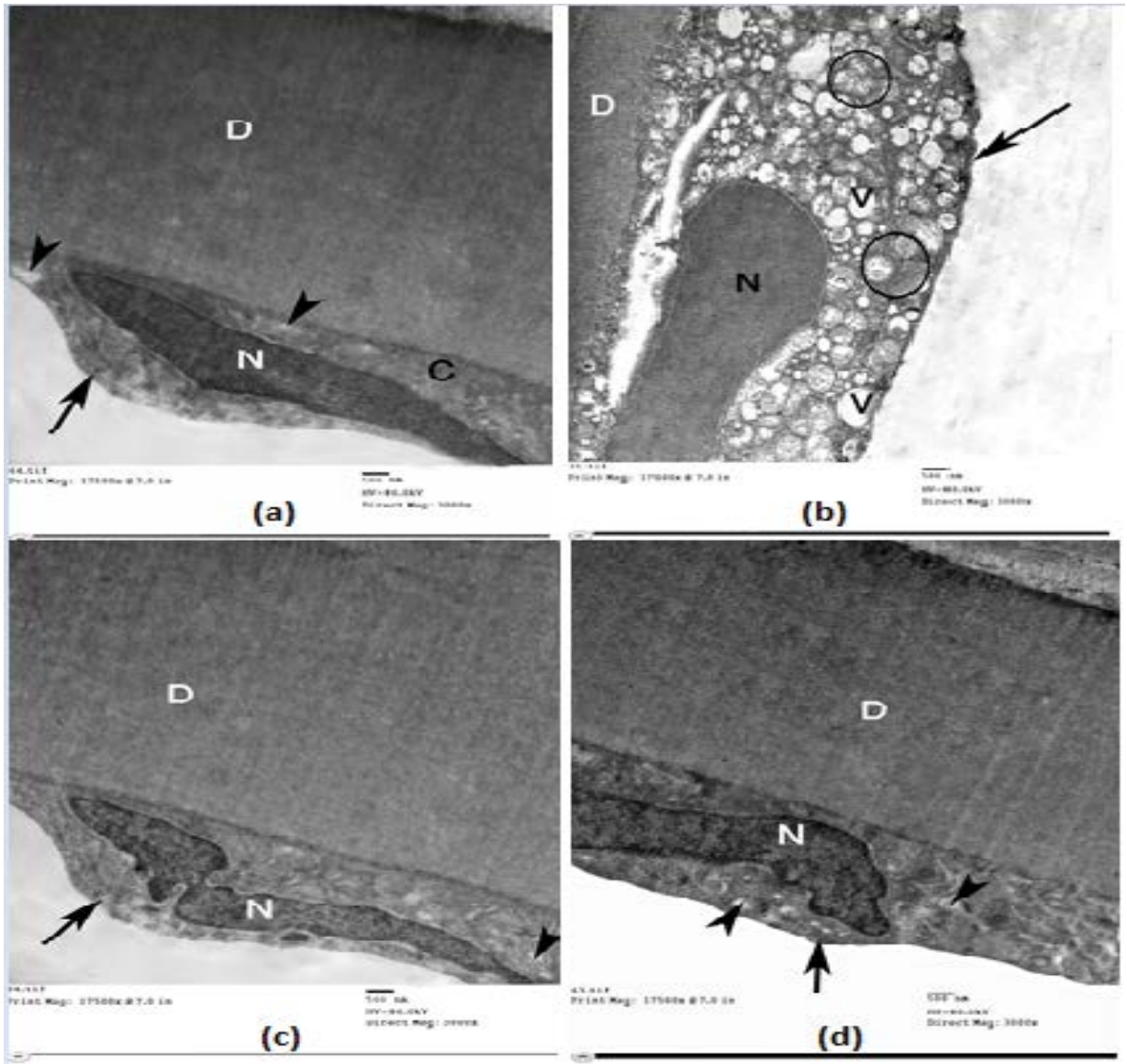


**Figure 7: (a)** An electron micrograph of a section in the cornea of Group I showing a thick homogenous electron-dense noncellular Descemet's membrane (D) and endothelial cells (black arrow ↑). Notice endothelial cell layer with a moderate electron-dense nucleus (N) and cytoplasm (C) with variable-sized pinocytotic vesicles (arrow heads ▲) **(TEM, × 3000)**; **(b)** An electron micrograph of a section in the cornea of Group II showing part of Descemet's membrane (D) and swollen endothelial cell (black arrow ↑). The endothelial cell has many variable-sized cytoplasmic vacuoles (V), degenerated mitochondria (circle), and an electron-dense elongated nucleus (N) **(TEM, × 3000)**; **(c)** An electron micrograph of a section in the cornea of Group III showing thick homogenous electron-dense Descemet's membrane (D) and endothelial cell (black arrow ↑). Notice endothelial cell with elongated nucleus (N) and variable-sized pinocytotic vesicles (arrow heads ▲) **(TEM, × 3000)**; **(d)** An electron micrograph of a section in the cornea of Group IV showing thick homogenous electron-dense Descemet's membrane (D). Notice nearly normal endothelial cell (black arrow ↑) with electron-dense elongated nucleus (N) and variable-sized pinocytotic vesicles (arrow heads ▲) **(TEM, × 3000)**.

| | Group I | Group II | Group III | Group IV |
|---|---|---|---|---|
| Mean area % | 293.64% | 186.30% | 282.55% | 287.22% |
| SD ± | 3.0351 | 7.3164 | 5.1982 | 3.0959 |
| Significance (sig.) at P<0.01 | 2 | 1,3,4 | 2 | 2 |
| 1=Significant with group I; 2=Significant with group II<br>3=Significant with group III; 4=Significant with group IV | | | | |

**Table 2:** Showing the mean and ± SD of corneal epithelium thickness (in pixels) for all groups with comparison between all groups by Post Hoc LSD test.

for innate immunity. Macrophages enhance serial steps of inflammation and have a vital role in corneal inflammatory disease due to release of various proinflammatory cytokines such as IL-1β, IL-6, IL-10, and TNF [35-38].

Macrophages release inflammatory mediators that lead to appearance of pathologically induced new blood vessels, a process known as CNV. CNV is frequently accompanied with serious drawbacks as wide stromal spaces known as corneal edema may contain edema fluids, inflammatory cellular infiltrates and secondary corneal scarring with elevated interstitial pressure, finally influencing corneal transparency and leading to loss of vision [35]. Some former workers [3,35] demonstrated the existence of CNV owing to disturbance in balance between several angiogenic factors such as fibroblast growth

| Gene | Group I | | | Group II | | | Group III | | | Group IV | | |
|---|---|---|---|---|---|---|---|---|---|---|---|---|
| | M | SD | Sig. | M | SD | Sig. | M | SD | Sig. | M | SD | Sig. |
| IL-1β | 0.49 | 0.2216 | b | 1.8 | 0.4348 | a,c,d | 0.74 | 0.3604 | b | 0.51 | 0.1923 | b |
| TNF-α | 0.32 | 0.1852 | b | 1.56 | 0.5047 | a,c,d | 0.57 | 0.3799 | b | 0.45 | 0.2536 | b |
| VEGF | 0.19 | 0.0471 | b,c,d | 1.06 | 0.1838 | a,c,d | 0.75 | 0.0981 | a,b,d | 0.34 | 0.1265 | a,b,c |
| a=Significant with group I; b=Significant with group II; c=Significant with group III; d=Significant with group IV; Significance at P<0.01 | | | | | | | | | | | | |

**Table 3:** Showing the mean (M) and ± SD of the IL-1β, TNF-α and VEGF genes expression in groups I, II, III and IV with comparison between the groups by Post Hoc LCD test.

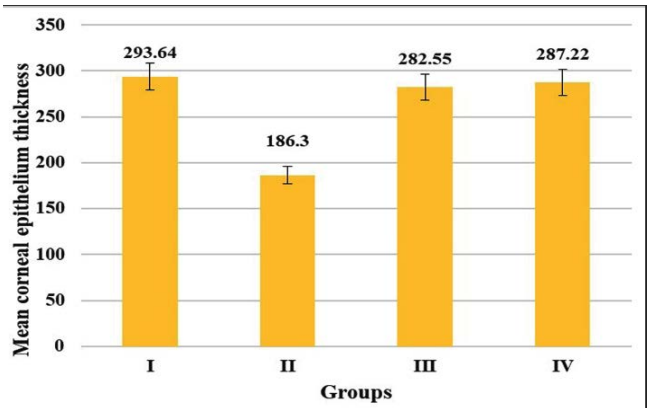


**Histogram 1:** Showing the means and ± SD of corneal epithelial thickness/ pixels.

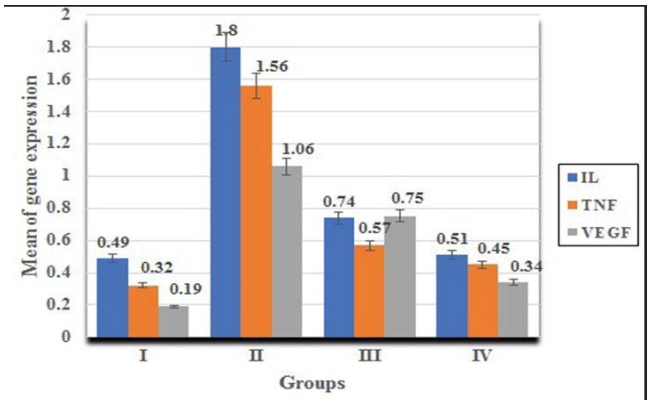


**Histogram 2:** Showing the mean of the IL-1β, TNF-α, and VEGF genes expression in all groups.

factor and Vascular Endothelial Growth Factor (VEGF) with a lot of anti-angiogenic molecules such as angiostatin, endostatin, and pigment epithelium derived factor in the cornea.

Our findings are also in agreement with other investigators [39] who mentioned that the wide intercellular spaces are due to disruption in desmosomes in epithelial cells of the deep layers. Meanwhile, disarrangement, destruction, and loss of collagen fibers are explained by apoptosis and loss of keratocytes responsible for collagen synthesis [3,14,40].

Alkali burns induced ulcers could be caused through production of Reactive Oxygen Species (ROS) in the corneas such as superoxide anion ($O_2^-$), hydrogen peroxide ($H_2O_2$), and hydroxyl radical (OH). They are produced by leukocytes and the respiratory mitochondrial chain. ROS share in many vital cellular operations such as cell proliferation, differentiation, and inflammation. These ROS of oxidative stress increase lipid peroxidation (Malondialdehyde (MDA)) which induces the disorder of the mitochondrial permeability transition pore and obstruct electron transfer, finally leading to apoptosis or necrosis. However, ROS can trigger the inflammation through the release of inflammatory cytokines, the expression of VEGF, and MMPs [36,41].

The promising healing properties of ADSCs have been considered valuable and ideal in regenerative therapies for several reasons. Meanly, they have great possibility for differentiation into mature cells along the endodermal, ectodermal and mesodermal lineage. They can be harvested and expanded in less invasive, simple, and more efficacious manner [9].

Group III of the current study revealed improvement of the histological changes with significant increase of corneal epithelial thickness and significant decrease of IL-1β, TNF, and VEGF genes expression as quantitated by RT-PCR in corneal tissue compared to Group II. Ultra-structural examination showed nearly normal superficial squamous cell with flat nucleus and apical microvilli, but the basal cells were nearly normal. The substantia propria of this group showed narrow spaces in between regularly arranged collagen fibers with nearly normal keratocyte. Descemet's membrane was lined with a nearly normal endothelial cell.

Sub-conjunctival injection of ADSCs was one of the most famous clinical management routes because it is a simple and easily used route for the ophthalmologists and thus we could use it in our study [42].

Our results showed homing of PKH26 labelled ADSCs to the site of injury, promoting repair of the injured cornea which corroborates the former reports on MSCs permeation after sub-conjunctival and systemic administration [43-45].

The results of our research were identical to the previous reports [46-48], which proved that ADSCs enhance corneal epithelial and stromal wound healing after alkali burns injuries through ameliorating inflammation by their anti-inflammatory effects and modulating immunity. Other studies stated that ADSCs had the ability to exert paracrine effects by secretion of antioxidant enzymes and many different cytokines besides their anti-apoptotic and anti-scarring properties. Also, they differentiate into the corneal epithelial or stromal cells in different types of corneal injury models as chemically burned corneas of rabbits [9,49,50].

Many studies explained that MSCs [51,52] act as a good stimulator for angiogenesis and could secrete vascular VEGF in an ischemia or tumor model. However, MSCs appeared to have a contradictory result in corneal angiogenesis. Some *in vivo* researchers [51,52] found that applying MSCs into the cornea could efficiently inhibit inflammation-related angiogenesis after induced chemical injury through their capacity to increase the liberation of thrombospondin-1, a powerful

anti-angiogenic factor. Also, many inflammation-related proangiogenic factors were significantly reduced after MSCs treatment.

Collectively, ADSCs therapeutic effects could be caused by a combination of multiple mechanisms, including anti-inflammatory, anti-apoptotic, anti-scarring, and finally paracrine effects.

Stem cell-based therapy has developed as a favourable approach for treating many diseases. Yet, it has a few disadvantages, like the need for a constant supply of cells, high cost, and time delays for the generation and handling of these cells. Additionally, issues correlated to ectopic tissue development and cellular rejection or unwanted engraftments have been reported [53].

In our research, Group IV showed marked recovery of the histological alterations with significant increase in corneal epithelial thickness and significant decrease in IL-1β, VEGF, and TNF genes expression as quantitated by RT-PCR in corneal tissue compared to Group II, while ultra-structural examination showed a nearly normal superficial squamous cell with flat nucleus and apical microvilli and electron-dense desmosomes connecting cells together with narrow intracellular space and also the basal cells were nearly normal. The cornea stroma of this group showed regularly arranged collagen fibers with nearly normal keratocyte. Descemet's membrane was lined with nearly normal endothelial cell.

Exosomes are promising as a controllable, manageable, and practical approach in future researches and clinical therapy [54]. Previous investigators [15] demonstrated that exosomes may be involved in the histological and ultra-structural changes of corneal epithelial cells and keratocytes so they can modify their activities. It is accepted by many authors [51,55] that they may play an important role in the regulation of numerous physiological processes through promoting secretion of anti-inflammatory cytokines, decreasing angiogenesis by reduction of VEGF, immune activation, regenerative capacities, and cell plasticity.

The equilibrium between angiogenic and anti-angiogenic factors in the corneal epithelium must be firmly controlled to preserving corneal avascularity. Exosomes carried proteins relevant to wound healing and NV including thrombospondin-2, which may be specially expressed on avascular tissues such as the cornea and participated in a lot of cellular events [15,56].

Some investigators [57] recommended that the enormous quantities of exosomes used in the MSCs-EX based therapies may have an important role in their mechanisms of action and make them efficient enough over the stem cells to suppress endogenous cytokines and other pathological factors released as a result of various induced injuries.

MSCs-EX have many characteristic advantages over stem cells as administration of exosomes is safer than stem cells; furthermore, their nano-dimensional size can allow them to easily cross through biological barriers and enter target organs. Also, exosomes can be stored without losing their function. All the previous described advantages make the curative application of exosomes more preferable than stem cells [17,18,58]. On the other hand, regardless of the numerous clinical trials on the application of exosomes in regenerative therapy, there are still some queries that can be topics of upcoming studies. What are the suitable and secure methods for the enormous production of the exosomes for clinical approaches? Which cell types are more suitable as exosome donor cells? So, there is an urgent need to carefully examine the subsequent features of exosomes: natural therapeutic potential, biogenesis mechanism, circulation kinetics, and biodistribution [59].

## Conclusion

ADSCs and exosomes can improve corneal alkali burn injuries and prevent their complications through anti-inflammatory and anti-angiogenic roles. MSCs-EX are a very promising approach and are considered better than ADSCs as they are safer than stem cells and their nano-dimension can easily cross through biological barriers and enter target organs.

### Conflicts of interest

There are no conflicts of interest.

### References

1. Ma XY, Bao HJ, Cui L, Zou J (2013) The graft of autologous adipose-derived stem cells in the corneal stromal after mechanic damage. PLoS ONE 8: 1-12. [PubMed]
2. Pescosolido N, Barbato A, Rusciano D (2015) Neovascularization in alkali-burned rabbit cornea. Clin Exp Ophthalmol 6: 1-5.
3. Soliman ME, Mahmoud BL, Kafafy MA (2015) Histological changes in cornea following repeated exposure to benzalkonium chloride and the possible protective effect of topically applied sodium hyaluronate. Nat Sci 13: 64-76.
4. Ravi KU (2017) Corneal defects and stem cell therapeutics. Glob J Intellect Dev Disabil 3: 1-20.
5. Filobbos SA, Abd El-Aziz DH, Mostafa MH (2016) Effect of subconjunctival injection of mesenchymal stem cells on alkali-induced acute corneal injury in rats. Med J Cairo Univ 84: 303-310.
6. Gao M, Sang W, Liu F (2016) High MMP-9 expression may contribute to retro prosthetic membrane formation after kpro implantation in rabbit corneal alkali burn model. J Ophthalmol 2016: 1-8.
7. Barboza MC, Barboza GC, Felberg S (2014) Induction of corneal collagen cross-linking in experimental corneal alkali burns in rabbits. Arq Bras Oftalmol 77: 310-314. [PubMed]
8. Chen Y, Yang W, Zhang X (2016) MK2 inhibitor reduces alkali burn induced inflammation in rat cornea. Sci Rep 6: 1-11.
9. Frese L, Dijkman PE, Hoerstrup SP (2016) Adipose tissue-derived stem cells in regenerative medicine. Transfus Med Hemother 43: 268-274. [PubMed]
10. Omar AI (2016) Influence of rat adipose tissue-derived mesenchymal stem cells on brain tissues following permanent unilateral common carotid artery occlusion in adult male albino rat: a histological and immunohistochemical study. EJH 39: 241-259.
11. Chen G, Jin Y, Shi X (2015) Adipose-derived stem cell-based treatment for acute liver failure. Stem Cell Res Ther 6: 1-11.
12. Wang J, Guo S, Liu X (2015) Protective effects of adipose-derived stem cells secretome on human dermal fibroblasts from ageing damages. Int J Clin Exp Pathol 8: 15739-15748. [PubMed]
13. Omar FR, Amin NMA, Elsherif HA (2016) Role of adipose-derived stem cells in restoring ovarian structure of adult albino rats with chemotherapy-induced ovarian failure: a histological and immunohistochemical study. J Carcinog Mutagen 7: 1-12.
14. Faruk EM, Mansy AE, Al-Shazly AM (2017) Light and electron microscopic study of the anti-inflammatory role of mesenchymal stem cell therapy in restoring corneal alkali injury in adult albino rats. J Stem Cell Bio Transplant 1: 1-11.
15. Han KY, Tran JA, Chang JH (2017) Potential role of corneal epithelial cell-derived exosomes in corneal wound healing and neovascularization. Sci Rep 7: 1-14. [PubMed]
16. Mead B, Tomarev S (2017) Bone Marrow-Derived mesenchymal stem cells-derived exosomes promote survival of retinal ganglion cells through mi RNA-dependent mechanisms. Stem Cells Transl Med 6: 1273-1285. [PubMed]
17. Yu B, Shao H, Su S (2016) Exosomes derived from MSCs ameliorate retinal laser injury partially by inhibition of MCP-1. Sci Rep 6: 1-12.
18. Omar SS (2017) Mesenchymal Stem Cells for Treating Ocular Surface Diseases. J Stem Cell Res 1: 1- 6.
19. Salem M, Helal O, Metwaly H (2017) Histological and immunohistochemical

study of the role of stem cells, conditioned medium and microvesicles in treatment of experimentally induced acute kidney injury in rats. Med J Cairo Univ 1: 70-83.

20. Sayed AA, EL-Deek SE, EL-Baz MA (2017) Exosomes derived from bone marrow mesenchymal stem cells restore cisplatin induced ovarian damage by promoting stem cell survival, meiotic, and apoptotic markers. Glo Adv Res J Med Med Sci 6: 116-130.
21. Bunnell BA, Flaat M, Gagliardi C (2008) Methods 45: 115-20.
22. Nassar W, El-Ansary M, Sabry D (2016) Umbilical cord mesenchymal stem cells derived extracellular vesicles can safely ameliorate the progression of chronic kidney diseases. Biomater Res 20: 1-11. [PubMed]
23. Tamura R, Uemoto S and Tabata Y (2016) Immunosuppressive effect of mesenchymal stem cell-derived exosomes on a concanavalin A-induced liver injury mode. Inflamm Regen 36: 1-12. [PubMed]
24. Hajrasouliha AR, Jiang G, Lu Q (2013) Exosomes from retinal astrocytes contain antiangiogenic components that inhibit laser-induced choroidal neovascularization. J Biol Chem 288: 28058- 28067. [PubMed]
25. Ahmed SK, Soliman AA, Omar SM (2015) Bone marrow mesenchymal stem cell transplantation in a rabbit corneal alkali burn model (A histological and immune histochemical study). Int J Stem Cells 8: 69-78. [PubMed]
26. Lin HF, Lai YC, Tai CF (2013) Effects of cultured human adipose-derived stem cells transplantation on rabbit cornea regeneration after alkaline chemical burn. Kaohsiung J Med Sci 29: 14-18. [PubMed]
27. Bai L, Shao H, Wang H (2017) Effects of Mesenchymal Stem Cell-Derived Exosomes on Experimental Autoimmune Uveitis. Sci Rep 7: 1-11. [PubMed]
28. Bancroft JD, Layton C (2013) The hematoxylin and eosin, connective and mesenchymal tissues with their stains. In: Suvarna SK, Layton C, Bancroft JD (eds.) Bancroft's theory and practice of histological techniques. 7th Edn. Philadelphia: Churchill Livingstone, pp. 173-212.
29. Hayat MA (2000) Chemical fixation. In: Hayat MA. (ed.) Principles and techniques of electron microscopy: biological applications. 4th Edn. Edinburg, UK: Cambridge University Press, pp. 4-85.
30. Sabry D, Noh O, Samir M (2016) Comparative evaluation for potential differentiation of endothelial progenitor cells and mesenchymal stem cells into endothelial-like cells. Int J Stem Cells 9: 44-52. [PubMed]
31. Li WJ, Hu YK, Song H (2016) Observation on ultrastructure and histopathology of cornea following femtosecond laser-assisted deep lamellar keratoplasty for acute corneal alkaline burns. Inter J Opthalmol 9: 481-486. [PubMed]
32. Beyazyildiz E, Pınarli FA, Beyazyildiz O (2012) A modified rat model for corneal alkali burn. Niche (31): 1- 3.
33. Kim DW, Lee SH, Shin MJ (2015) PEP-1-FK506BP inhibits alkali burn-induced corneal inflammation on the rat model of corneal alkali injury. BMB Rep 48: 618-623. [PubMed]
34. Bermudez ML, Lago S, Eiro N (2015) Corneal epithelial wound healing and bactericidal effect of conditioned medium from human uterine cervical stem cells. Invest Ophthalmol Vis Sci 56: 983-992. [PubMed]
35. El-Fattah El-Shazly AA, Ahmed AI (2016) Therapeutic effects of extracts from spirulina platensis versus bevacizumab on inflammation-associated corneal neovascularization. J Med Surg Pathol 1: 1-7.
36. Gu XJ, Liu X, Chen YY (2016) Involvement of NADPH oxidases in alkali burn-induced corneal injury. Int J Mol Med 38: 75-82. [PubMed]
37. Zhong J, Deng J, Tian B (2016) Hyaluronate acid-dependent protection and enhanced corneal wound healing against oxidative damage in corneal epithelial cells. J Ophthal 2016: 1-10.
38. Liu J, Xue Y, Dong D (2017) CCR2- andCCR2+ corneal macrophages exhibit distinct characteristics and balance inflammatory responses after epithelial abrasion. Mucosal Immunol 10: 1145-1159.
39. Kalleny NK, Soliman NBE (2011) Light and electron microscopic study on the effect of topically applied hyaluronic acid on experimentally induced corneal alkali burn in albino rats. EJH 34: 829-848.
40. Mohamed SH (2012) Light and electron microscopic study of the corneal stroma during the healing process of alkali-induced ulcer. EJH 35: 67-73.
41. Bashkaran K, Zunaina E, Bakiah S (2011) Anti-inflammatory and antioxidant effects of Tualang honey in alkali injury on the eyes of rabbits: Experimental animal study. BMC Complement Altern Med 11: 1-11. [PubMed]
42. Tsuji W, Rubin JP, Marra KG (2014) Adipose-derived stem cells: Implications in tissue regeneration. World J Stem Cells 6: 312-321. [PubMed]
43. Cejka C, HolanV, Trosan P (2016) The favorable effect of mesenchymal stem cell treatment on the antioxidant protective mechanism in the corneal epithelium and renewal of corneal optical properties changed after alkali burns. Oxid Med Cell Longev 2016: 1-12. [PubMed]
44. Lan Y, Kodati S, Lee HS (2012) Kinetics and function of mesenchymal stem cells in corneal injury. Invest Ophthalmol Vis Sci 53: 3638-3644. [PubMed]
45. Zickri MB, Ahmad NA, El Maadawi ZM (2012) Effect of stem cell therapy on induced diabetic keratopathy in albino rat. Int J Stem Cells 5: 57-64. [PubMed]
46. Aly LAA, El-Menoufy H, Ragae A (2012) Adipose stem cells as alternatives for bone marrow mesenchymal stem cells in oral ulcer healing. Int J Stem Cells 5: 104-114. [PubMed]
47. Lin KJ, Loi MX, Lien GS (2013) Topical administration of orbital fat-derived stem cells promotes corneal tissue regeneration. Stem Cell Res Ther 4: 1-12. [PubMed]
48. Zeppieri M, Brusini P, Parodi PB (2015) Corneal treatment with adipose derived stem cells. Glo Adv Res J Med Med Sci 4: 296-300.
49. Beyazyildiz E, Pinarli FA, Beyazyildiz O (2014) Efficacy of topical mesenchymal stem cell therapy in the treatment of experimental dry eye syndrome model. Stem Cells Int 2014: 1- 9.
50. Aboul-Fotouh GI, Zickri MB, Metwally HG (2015) Therapeutic effect of adipose derived stem cells versus atorvastatin on amiodarone induced lung injury in male rat. Int J Stem Cells 8: 170-180. [PubMed]
51. Yao L, Bai H (2013) Review: Mesenchymal stem cells and corneal reconstruction. Mol Vis 19: 2237-2243. [PubMed]
52. Ghazaryan E, Zhang Y, He Y (2016) Mesenchymal stem cells in corneal neovascularization: comparison of different application routes. Mol Med Rep 14: 3104-3112. [PubMed]
53. Lou G, Chen Z, Zheng M (2017) Mesenchymal stem cell-derived exosomes as a new therapeutic strategy for liver diseases. Exp Mol Med 49: 1-9. [PubMed]
54. Yu B, Zhang X and Li X (2014) Exosomes Derived from Mesenchymal Stem Cells. Int J Mol Sci 15: 4142-4157. [PubMed]
55. Vizoso FJ, Eiro N, Cid S (2017) Mesenchymal stem cell secretome: toward cell-free therapeutic strategies in regenerative medicine. Int J Mol Sci 18: 1-24. [PubMed]
56. Huang L, Ma W, Ma Y (2015) Exosomes in mesenchymal stem cells, a new therapeutic strategy for cardiovascular diseases? Int J Biol Sci 11: 238-245. [PubMed]
57. Shen B, Liu J, Zhang F (2016) CCR2 positive exosome released by mesenchymal stem cells suppresses macrophage functions and alleviates ischemia/reperfusion-induced renal injury. Stem Cells Int 2016: 1-9.
58. Rani S, Ryan AE, Griffin MD (2015) Mesenchymal stem cell-derived extracellular vesicles: toward cell-free therapeutic applications. Mol Ther 23: 812-823. [PubMed]
59. Cheng L, Zhang K, Wu S, Cui M (2017) Focus on mesenchymal stem cell-derived exosomes: opportunities and challenges in cell-free therapy. Stem Cells Int 2017: 1-10. [PubMed]